

Characterization of diketopiperazine heterodimers as potential chemical markers for discrimination of two dominant black aspergilli, *Aspergillus niger* and *Aspergillus tubingensis*

Ce Xu^{a,b,1}, Kuo Xu^{a,1}, Xiao-Long Yuan^a, Guang-Wei Ren^a, Xiao-Qiang Wang^a, Wei Li^c, Ning Deng^a, Xiu-Fang Wang^{a,**}, Peng Zhang^{a,*}

^a Tobacco Research Institute of Chinese Academy of Agricultural Sciences, Qingdao, 266101, People's Republic of China

^b Graduate School of Chinese Academy of Agricultural Sciences, Beijing, 100081, China

^c College of Marine Life Sciences, Ocean University of China, Qingdao, 266003, People's Republic of China

ARTICLE INFO

Keywords:

Aspergillus tubingensis Mosseray (discellaceae)
Black aspergilla
Chemotaxonomy
Diketopiperazine heterodimers
Asperazines
Antifungal activity

ABSTRACT

Black aspergilli are distributed worldwide and represent one of the most prolific sources of metabolites with biomedical and agrochemical interests. However, due to their similar morphological characteristics and insufficient molecular identification, the taxonomic classification of black aspergilli remains ill-defined. The production of specialised metabolites is often unique for species among black aspergilli and could be used as diagnostic chemical markers for species identification. In this study, chemical investigation of *Aspergillus tubingensis* OUCMBIII 143291 led to the discovery of the diagnostic chemical marker asperazine, a complex diketopiperazine heterodimer, as well as two previously undescribed analogues, asperazine B and C. In addition, an undescribed 2-benzylpyridin-4(1*H*)-one-containing amide, pestalamide D, along with four known related metabolites were isolated. Their chemical structures, including their absolute configurations, were established on the basis of comprehensive spectral analysis and chiral HPLC analysis of the acidic hydrolysates. Asperazines B and C can serve as potential chemical markers for distinguishing *A. tubingensis* from *A. niger*, two representative species of black aspergilli that are usually incorrectly identified. Moreover, the isolated compounds were evaluated for their antifungal activity against eight phytopathogenic fungi including *Alternaria alternata*, *A. brassicae*, *Botrytis cinerea*, *Colletotrichum lagenarium*, *Fusarium oxysporum*, *Gaeumannomyces graminis*, *Penicillium digitatum*, and *Valsa mali*. Pestalamide D exhibited significant activities against *B. cinerea*, *C. lagenarium*, and *V. mali*, with MIC values of 4, 8, and 8 µg/mL, respectively, compared with the positive controls carbendazim (MICs = 8, 4, and 4 µg/mL) and prochloraz (MICs = 8, 8, and 4 µg/mL). The results of this study reveal two additional chemical markers and provide a powerful tool for the rapid identification of black aspergilli.

1. Introduction

The *Aspergillus* (Aspergillaceae) genus has been well studied and proved to be the predominant producer of diverse specialised metabolites with high economic, agronomic, and/or medical importance. The section *Nigri* within this genus, also known as black aspergilli, comprises 26 closely related species (e.g., *A. acidus*, *A. aculeatus*, *A. brasiliensis*, *A. carbonarius*, *A. heteromorphus*, *A. ibericus*, *A. lacticoffeatus*, *A. japonicus*, *A. niger*, *A. tubingensis*) that have mainly been isolated from soil and plant sources (Varga et al., 2011; Xanthopoulou et al., 2019). They are an important group in the food mycology and biotechnology

industries for the production of extracellular or intracellular enzymes (such as amylases and lipases), organic acids (such as citric acid and gluconic acid), and antibiotics in food fermentation processes (Samson et al., 2007; Varga et al., 2011). Besides their economic importance, many species can cause food spoilage and contamination by synthesizing mycotoxins (such as ochratoxin A and fumonisins) (D'hooge et al., 2019). Among the described species, *A. niger* (Moniliaceae) and *A. tubingensis* (Discellaceae) are the most representative species of black aspergilli (Mirhendi et al., 2016). *A. niger* is ubiquitous in soil and may cause black mould on certain fruits and vegetables, such as grapes, onions, and peanuts (Abdel-Aziz et al., 2019), while *A. tubingensis* is

* Corresponding author.

** Corresponding author.

E-mail addresses: wangxiufang02@caas.cn (X.-F. Wang), zhangpeng@caas.com (P. Zhang).

¹ These authors contributed equally to this work.

frequently responsible for the postharvest decay of some economic fruits and vegetables (Apaliya et al., 2017; Perrone et al., 2007).

Although the section *Nigri* of *Aspergillus* has been studied for nearly 90 years (the first species was discovered by Raoul Mosseray in 1934), taxonomic classification in the *Nigri* section is a remaining challenge (D'hooge et al., 2019). Due to their extremely similar morphological characteristics and insufficient molecular identification, distinguishing these species is difficult and, in many cases, has resulted in misclassifications and conflicting phylogenetic trees (Nielsen et al., 2009). The taxonomic classification of black aspergilli can be successfully achieved based on a combination of phenotypic, chemotaxonomic, molecular and chromatographic approaches (Xanthopoulou et al., 2019). New molecular DNA-based techniques for rapid and accurate differentiation, such as amplified fragment length polymorphism (AFLP), restriction fragment length polymorphism (RFLP), random amplified polymorphic DNA (RAPD), and multilocus sequence typing (MLST), have been investigated and applied in recent years (Xanthopoulou et al., 2019). Alternatively, unique chemical markers provide an efficient chemotaxonomic methodology to identify these closely-related species (Nielsen et al., 2009). Asperazine, an unusual unsymmetrical diketopiperazine dimer isolated from *A. tubingensis* was proposed as a distinctive chemical marker to distinguish *A. tubingensis* from *A. niger* (Choque et al., 2018; Nielsen et al., 2009). Genomic analyses revealed that *A. tubingensis* has the capacity to produce asperazine, while none of the *A. niger* strains possessed this capacity (Choque et al., 2018). Recently, we isolated *A. tubingensis* from intertidal zone sediment. To satisfy our curiosity that whether this strain can produce the chemical marker asperazine or its derivatives, we performed chemical investigation of this fungal strain. As a result, asperazine (1) and two undescribed analogues, asperazine B (2) and C (3), were subsequently isolated and identified (Fig. 1). Asperazines B (2) and C (3) provided additional chemical markers for distinguishing *A. tubingensis* and other related species of black aspergilli. In addition, an undescribed 2-benzylpyridin-4(1H)-one-containing amide, pestalamide D (4), and four known related metabolites (5–8) were also isolated (Fig. 1). In the present study, we reported the isolation, structure

determination, chemotaxonomic significance, and antifungal activity of these compounds.

2. Results and discussion

2.1. Structural elucidation of the isolated compounds

Compound 2 was isolated as a white amorphous powder. Its molecular formula was determined to be $C_{40}H_{36}N_6O_5$ from the prominent ESI HRMS peak at m/z 681.2812 $[M + H]^+$ (calcd. 681.2820), which was in accordance with the 1H and ^{13}C NMR data. Detailed analysis of the 1H , ^{13}C , and HSQC NMR spectroscopic data of 2 (Table 1) revealed the presence of four methylenes, five sp^3 methines, one quaternary carbon, 26 aromatic/olefinic carbons (17 of which were protonated), and four amide carbonyls. Moreover, the 1H NMR spectrum showed additionally six exchangeable protons [δ_H 6.65 (s, 1-NH), 8.19 (s, 14-NH), 9.64 (s, 30-NH), 7.88 (s, 35-NH), 7.96 (s, 38-NH), and 9.27 (s, 44-OH)] in $DMSO-d_6$. Comparison of the 1D NMR spectroscopic data of 2 with those of asperazine (1) revealed their structural similarities (Varoglu et al., 1997). The main differences were the 16 additional mass units in the molecular weight of 2, as well as the presence of an oxygenated sp^2 quaternary carbon (δ_C 156.1, C-44) in 2, suggesting that 2 is also a diketopiperazine heterodimer equivalent to 1 with the substitution of a phenylalanine (Phe) unit for tyrosine (Tyr) in one of the monomeric subunits (Ding et al., 2008). The key 1H - 1H COSY and HMBC data of 2 further confirmed the presence of the Tyr residue (Fig. 2). Interpretation of the selected HMBC correlations from H-2 to C-3, C-4, C-12, and C-24; from H-12 to C-3, C-4, and C-24; and from H-25 to C-3 established a linkage envisioned between C-3 and C-24, which was previously reported in asperazine (Varoglu et al., 1997) and pestalazine A (Ding et al., 2008) but was different from that in the C^3,N^{30} -connected asperazine A (Li et al., 2015), cristatumin E (Li et al., 2013), WIN 64821 and WIN 64745 (Barrow et al., 1993; Ovenden et al., 2004). Accordingly, the collective 1D and 2D NMR data allowed the gross structure of 2 to be assembled as shown in Fig. 1.

The NOESY experiment was applied to assign the relative

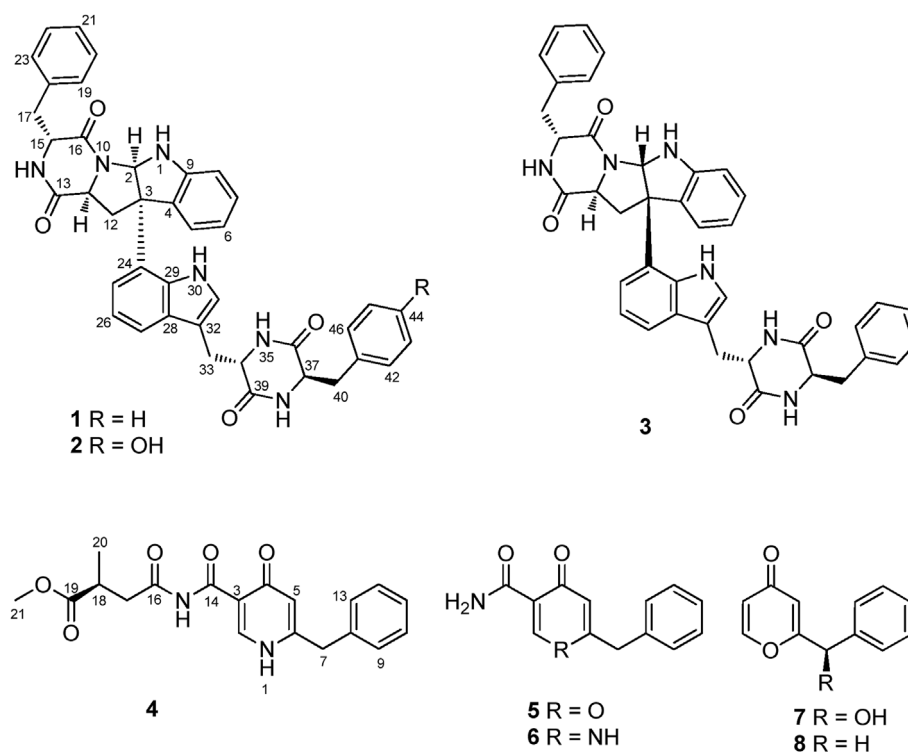


Fig. 1. Structures of compounds 1–8.

Table 1
 ^1H (500 MHz) and ^{13}C NMR (125 MHz) data of compounds **2** and **3** in $\text{DMSO-}d_6$

No.	Compound 2		Compound 3	
	δ_{H} (mult, J in Hz)	δ_{C} , type	δ_{H} (mult, J in Hz)	δ_{C} , type
1-NH	6.65 (1H, s)		7.22 (1H, s)	
2	5.83 (1H, s)	82.0, CH	5.71 (1H, s)	79.1, CH
3		57.0, C		57.3, C
4		132.2, C		130.8, C
5	6.77 (1H, d, 7.5)	123.6, CH	7.04 (1H, overlap)	123.6, CH
6	6.53 (1H, t, 7.5)	118.3, CH	6.59 (1H, t, 7.5)	119.0, CH
7	7.01 (1H, overlap)	128.3, CH	6.94 (1H, overlap)	128.5, CH
8	6.69 (1H, t, 7.5)	110.2, CH	6.71 (1H, d, 7.5)	110.0, CH
9		147.5, C		148.7, C
11	3.40 (1H, overlap)	56.0, CH	3.90 (1H, dd, 12.0, 4.5)	55.6, CH
12a	3.07 (1H, overlap)	37.8, CH_2	3.03 (1H, overlap)	36.4, CH_2
12b	2.24 (1H, t, 12.0)		1.90 (1H, t, 12.0)	
13		168.3, C		167.4, C
14-NH	8.19 (1H, s)		8.14 (1H, s)	
15	4.02 (1H, m)	58.2, CH	4.44 (1H, m)	58.2, CH
16		166.9, C		165.0, C
17a	3.04 (1H, overlap)	38.6, CH_2	3.04 (1H, overlap)	38.8, CH_2
17b	2.88 (1H, overlap)		2.98 (1H, 14.0, 3.5)	
18		136.0, C		136.6, C
19, 23	7.03 (2H, overlap)	129.5, CH	6.98 (2H, overlap)	129.7, CH
20, 22	7.04 (2H, overlap)	128.3, CH	6.99 (2H, overlap)	128.0, CH
21	7.12 (1H, t, 7.5)	126.9, CH	7.14 (1H, overlap)	126.4, CH
24		123.2, C		126.6, C
25	6.92 (1H, overlap)	118.5, CH	6.93 (1H, overlap)	118.0, CH
26	6.98 (1H, overlap)	118.4, CH	6.96 (1H, overlap)	118.4, CH
27	7.53 (1H, d, 7.5)	118.7, CH	7.45 (1H, d, 7.5)	118.6, CH
28		129.1, C		128.7, C
29		132.8, C		132.5, C
30-NH	9.64 (1H, s)		10.24 (1H, s)	
31	6.97 (1H, overlap)	124.9, CH	7.03 (1H, overlap)	124.7, CH
32		108.9, C		109.0, C
33a	3.11 (1H, overlap)	27.9, CH_2	3.08 (1H, overlap)	28.2, CH_2
33b	2.84 (1H, overlap)		2.85 (1H, dd, 15.0, 5.0)	
34	3.35 (1H, overlap)	54.3, CH	3.36 (1H, overlap)	54.7, CH
35-NH	7.88 (1H, s)		7.97 (1H, s)	
36		167.6, C		167.6, C
37	3.42 (1H, overlap)	55.1, CH	3.45 (1H, overlap)	54.5, CH
38-NH	7.96 (1H, s)		7.93 (1H, s)	
39		167.1, C		167.0, C
40a	2.90 (1H, overlap)	37.1, CH_2	2.97 (1H, overlap)	37.6, CH_2
40b	2.60 (1H, dd, 13.5, 4.5)		2.71 (1H, dd, 13.5, 5.0)	
41		125.8, C		136.1, C
42, 46	6.62 (2H, d, 8.0)	131.1, CH	7.10 (2H, overlap)	130.1, CH
43, 45	6.90 (2H, d, 8.0)	114.8, CH	7.20 (2H, overlap)	127.9, CH
44		156.1, C	7.13 (1H, overlap)	126.6, CH
44-OH	9.27 (1H, s)			

configuration of the diketopiperazine rings. In the NOESY spectrum, H-11 (δ_{H} 3.40) exhibited unambiguous correlated signals with H₂-17 (δ_{H} 3.04 and 2.88) but showed no correlation with H-15 (δ_{H} 4.02),

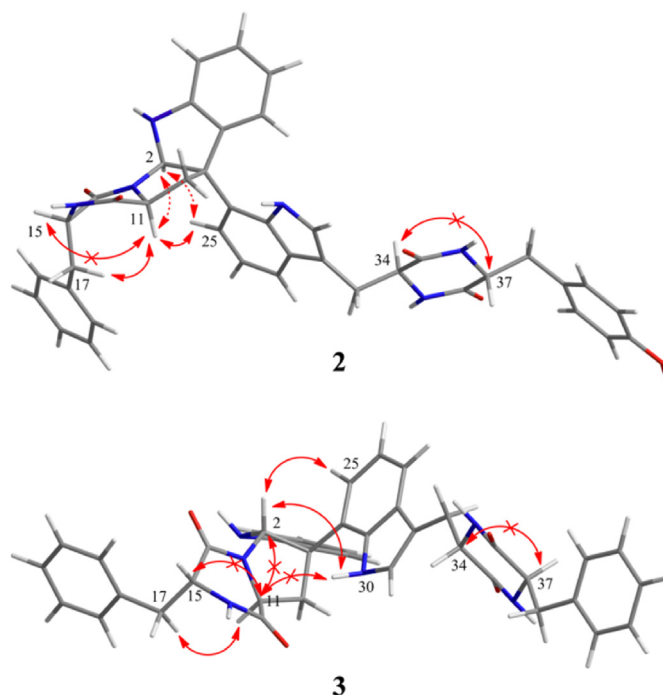


Fig. 3. Key NOESY correlations of compounds **2** and **3**.

indicating that H-11 and H₂-17 were on the same face of the diketopiperazine ring (Fig. 3). Additional NOESY correlations of H-11 with H-2 (δ_{H} 5.83) and H-25 (δ_{H} 6.92), and of H-2 with H-25, revealed that H-11, H-2, and the C-24 indole moiety were located on the same face of the pyrrolidine ring. The absence of correlated signals for H-34 (δ_{H} 3.35) with H-37 (δ_{H} 3.42) led to the tentative assignment of these two protons as having a *trans* configuration, which was supported by a biosynthetic analogy to the stereochemistry of H-11 and H-15 for asperazine and asperazine A (Varoglu et al., 1997; Ding et al., 2008).

The absolute configuration of **2** was determined by acidic hydrolysis and chiral HPLC analysis (Ding et al., 2008; Li et al., 2013; Zhang et al., 2015). The acidic hydrolysates of **2** and standard compounds, *D*- and *L*-Tyr, *D*- and *L*-Phe, were prepared and subjected to chiral HPLC analysis. The retention times of the hydrolysates of **2** (t_{R} 14.1 and 25.9 min) were the same as those of authentic *D*-Tyr (t_{R} 14.1) and *D*-Phe (t_{R} 25.9 min), respectively, but were different from those of authentic *L*-Tyr (t_{R} 21.6 min) and *L*-Phe (t_{R} 38.0) (Fig. 4), suggesting the presence of *D*-Tyr and *D*-Phe residues in **2**. Thus, the absolute configurations of **2** were defined as (2*R*, 3*R*, 11*S*, 15*R*, 34*S*, 37*R*).

Compound **3** was also isolated as a white amorphous powder. On basis of ESI HRMS analysis (m/z 665.2866 [$\text{M} + \text{H}$]⁺, calcd. 665.2871), the molecular formula of $\text{C}_{40}\text{H}_{36}\text{N}_6\text{O}_4$ was assigned. Analysis of the ^1H , ^{13}C and DEPT NMR data for **3** (Table 1) and its 2D

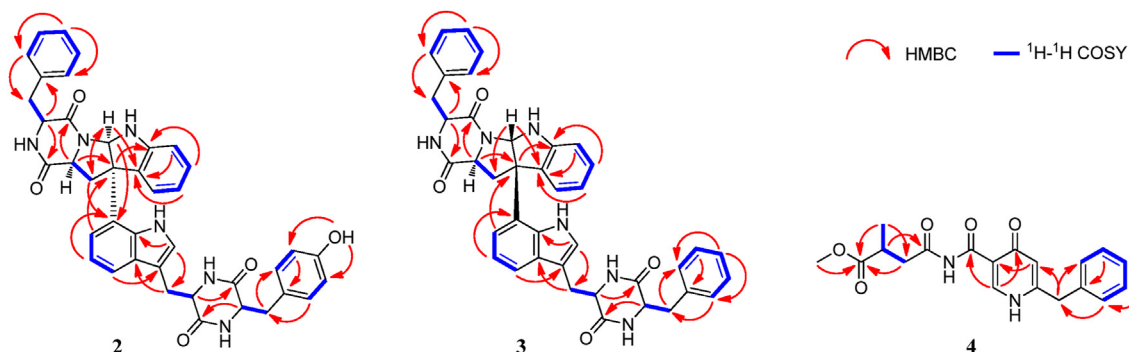


Fig. 2. Key HMBC and ^1H - ^1H COSY correlations of compounds **2**, **3**, and **4**.

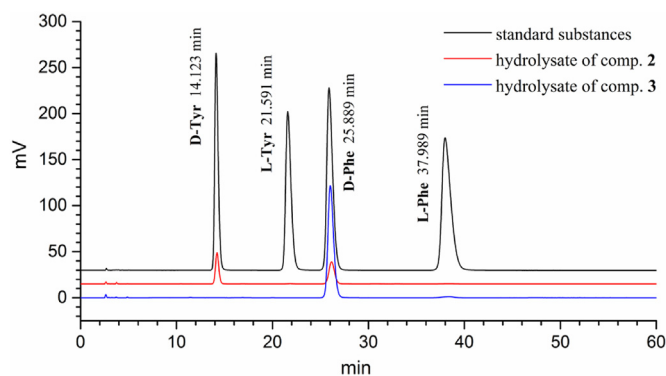


Fig. 4. The chiral HPLC analyses of the hydrolysates of compounds 2 and 3.

NMR spectra (Fig. 2) revealed that **3** has the same planar structure as asperazine (**1**) (Varoglu et al., 1997). However, the chemical shifts of the carbons surrounding the two chiral centers, C-2 and C-3, exhibited clear changes when measured in the same solvent, DMSO- d_6 . The chemical shifts of C-2 (δ_C 79.1), C-4 (δ_C 130.8), and C-12 (δ_C 36.4) of **3** were shifted upfield (δ_C 82.0, 132.2, 37.6 for **1**, respectively), while C-3 (δ_C 57.3) and C-24 (δ_C 126.6) were shifted downfield (δ_C 57.0 and 123.6 for **1**). These changes indicated that **3** was the C-2 and C-3 stereoisomer of **1**. In the NOESY experiment, H-11 (δ_H 3.90) exhibited unambiguous correlated signals with H₂-17 (δ_H 3.04), but showed no correlation with H-15 (δ_H 4.44). These results indicated that H-11 and CH₂-17 were on the same face of the diketopiperazine-ring, while H-15 was on the opposite side as in **1** and **2** (Fig. 3). Additional unambiguous NOESY correlations of H-2 (δ_H 5.71) with H-25 (δ_H 6.93) and H-30 (δ_H 10.24), as well as the absence of the correlated signals of H-11 (δ_H 3.90) with H-2 and H-30 revealed that H-2 and the C₂₄-indole moiety were located both on the other face of the pyrrolidine-ring. The absence of the correlated signals of H-34 (δ_H 3.36) with H-37 (δ_H 3.45) indicated that these two protons were in *trans*-positions as in **1** and **2**. To further determine the configurations of the amino acid residues, acidic hydrolysates of **3** were analyzed by chiral HPLC (Fig. 4), which showed the presence of D-Phe (t_R 25.9 min).

Compound **4** was isolated as colorless oil. Its molecular formula of C₁₉H₂₀N₂O₅ was established based on pseudomolecular ion peaks at m/z 357.1438 [M + H]⁺ (calcd. 357.1445) and 379.1255 [M + Na]⁺ (calcd. 379.1264) in the HRESIMS spectrum. In accordance with the proposed molecular formula, its ¹³C NMR data (Table 2) revealed the

Table 2
¹H (500 MHz) and ¹³C NMR (125 MHz) data of compound **4** in DMSO- d_6

No.	δ_H (mult, J in Hz)	δ_C , type
1	13.11 (1H, s)	
2	8.46 (1H, s)	143.9, CH
3		115.1, C
4		177.5, C
5	6.34 (1H, s)	118.6, CH
6		152.4, C
7	3.94 (2H, s)	37.9, CH ₂
8		136.8, C
9, 13	7.30–7.34 (2H, overlap)	128.7, CH
10, 12	7.32–7.36 (2H, overlap)	128.9, CH
11	7.27 (1H, m)	127.0, CH
14		163.3, C
15	12.75 (1H, s)	
16		173.0, C
17a	2.89 (1H, dd, 15.5, 8.5)	34.4, CH ₂
17b	3.14 (1H, dd, 15.5, 8.0)	
18	2.86 (1H, overlap)	41.3, CH
19		175.5, C
20	1.14 (3H, d, 6.5)	16.9, CH ₃
21	3.58 (3H, s)	51.5, CH ₃

presence of 19 carbons, which were classified as two methyls (including a methoxy group), two methylenes, one sp³ methine, and seven aromatic/olefinic methines, three aromatic/olefinic quaternary carbons, and four carbonyl carbons. The 1D NMR data were highly similar to those of pestalamide B, an amide containing a 2-benzylpyridin-4(1H)-one substructure previously isolated from the plant pathogenic fungus *Pestalotiopsis theae* (Ding et al., 2008). An additional methoxy group ($\delta_{H/C}$ 3.58/51.5, C-21) was observed in **4**, suggesting **4** as the methyl ester of pestalamide B. The absolute configuration of C-18 in **4** was assigned as *S* by comparison of its specific rotation ($[\alpha]_{25}^D$ -10, MeOH) with that of pestalamide B ($[\alpha]_{25}^D$ -8, MeOH). It is worth mentioning that specialised metabolites bearing 2-benzylpyridin-4(1H)-one have been encountered in relatively few fungi outside of the black aspergilli clade (Henrikson et al., 2011). Notably, to better understand the distribution of 2-benzylpyridin-4(1H)-ones among black aspergilli, Henrikson et al. analyzed 11 black aspergilli strains and found that pestalamide B was the only metabolite common to all 11 strains (Henrikson et al., 2011).

2.2. Study of chemotaxonomic significance

As mentioned above, black aspergilli species are phylogenetically closely related, and their taxonomic classification is challenging and has changed numerously in the last few decades (D'hooge et al., 2019; Samson et al., 2007; Varga et al., 2011). In general, fungal species can be distinguished by a combined polyphasic approach including evaluation of their morphological characteristics (colony morphology, conidial size, and ornamentation), biochemical properties, and molecular analysis (Bathoorn et al., 2013; D'hooge et al., 2019). Unfortunately, most of the species belonging to black aspergilli are morphologically indistinguishable. Diagnostic molecular DNA-based techniques, such as PCR-RFLP and RAPD-PCR, appear to be the most useful and effective methods to successfully facilitate correct species determination (Bathoorn et al., 2013).

In this study, we obtained two fungal strains, *A. niger* and *A. tubingensis*, and performed species identification based on morphological characteristics and molecular analysis. For the morphological characteristics, both strains possessed very similar microscopic characteristics, such as dark brown and spiny conidia, spherical vesicles, and lightly pigmented hyphae near the apex (Fig. 5) (Mirhendi et al., 2016). These two strains can be recognized as black aspergilli at only the genus level and cannot be distinguished from one another using morphological characteristics. Next, the strains were subjected to molecular re-identification. The ITS region, 18S and 26S rRNA genes were amplified and sequenced. Based on the sequences of the ITS rDNA and 18S and 26S rRNA regions, phylogenetic analyses showed that the two fungal strains of *A. niger* and *A. tubingensis* were placed in different evolutionary positions (Fig. 6). Therefore, the molecular identification of these fungal strains was too ambiguous to determine their taxonomic status.

The production of specialised metabolites is often unique for species within black aspergilli and could be used as diagnostic chemical markers for identification (Mirhendi et al., 2016). Since *A. tubingensis* was often misidentified as *A. niger*, very recently, whole-genome sequencing of *A. tubingensis* was carried out (Choque et al., 2018; Nielsen et al., 2009). The genomic analyses suggested that *A. tubingensis* has the capacity to produce asperazine (Choque et al., 2018). Comprehensive analysis of the specialised metabolites from 140 strains of *A. niger* revealed that none of the *A. niger* strains possessed the capacity to produce asperazine, proposing asperazine as a distinctive chemical marker to distinguish *A. tubingensis* from *A. niger* (Nielsen et al., 2009). This was also concluded on the basis of the genomic features of the putative secondary metabolite clusters classification for asperazine biosynthesis (Choque et al., 2018). Since the gene clusters might be silent, to evaluate the authentic capacity to produce asperazine, crude extracts of *A. tubingensis* and *A. niger* in PDB medium were analyzed by HPLC-DAD.

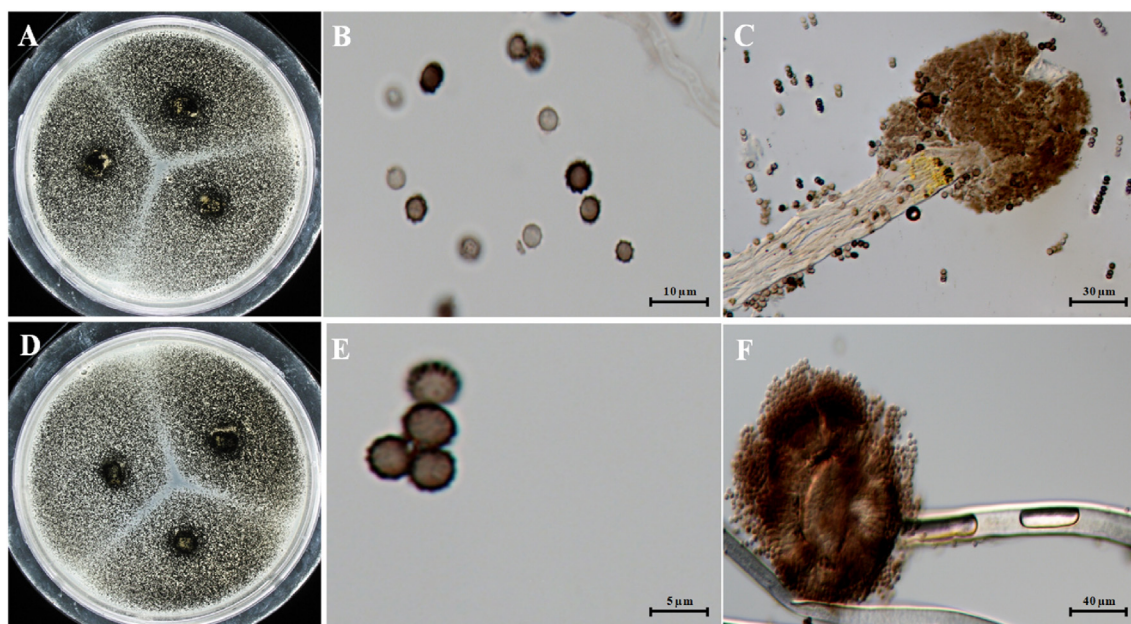


Fig. 5. Culture and morphological characteristics of *Aspergillus niger* (A) and *A. tubingensis* (D), colonies on PDA media; Conidia and conidiophores heads of *A. niger* (B–C) and *A. tubingensis* (E–F).

The results indicated that both species can produce dimeric naphtho- γ -pyrones, which represent the most abundant family of specialised metabolites in black aspergilli (Choque et al., 2014; Nielsen et al., 2009). However, the HPLC-DAD profile of *A. tubingensis* showed a prominent peak attributed to asperazine (Fig. 7). This is the first time to report asperazine isolated from *A. tubingensis*. Moreover, the isolation of two further asperazine derivatives may serve as additional chemical markers, which provide a powerful tool for the rapid identification of black aspergilli.

2.3. Antifungal activity

Microbial specialised metabolites served as a rich resource for exploring lead compounds with medicinal and/or agricultural importance (Cao et al., 2019). A previous study indicated the good performance of *A. tubingensis* as a potential biocontrol agent against grey mould on tomato caused by *Botrytis cinerea* (Zhao et al., 2018). Thus, the specialised metabolites of this strain might possess considerable antifungal activities and could be used as lead compounds with agrochemical significance. Compounds 1–8 were evaluated for their antifungal activity against eight widely distributed pathogenic fungi (*A. alternata*, *A. brassicae*, *B. cinerea*, *C. lagenarium*, *F. oxysporum*, *G. graminis*, *P. digitatum*, and *V. mali*). As shown in Table 3, compounds 2, 4, and 6 displayed potent and specific antifungal activity, with MIC values of 4 or 8 $\mu\text{g}/\text{mL}$. Compound 2 demonstrated strong activity against *V. mali* with an MIC value of 4 $\mu\text{g}/\text{mL}$, which was equal to that of the positive controls carbendazim and prochloraz (MICs = 4 $\mu\text{g}/\text{mL}$). Compound 4 exhibited significant activity against *B. cinerea*, *C. lagenarium*, and *V. mali*, with MIC values of 4, 8, and 8 $\mu\text{g}/\text{mL}$, respectively. Interestingly, compound 4 showed higher growth-inhibitory activity (MIC = 4 $\mu\text{g}/\text{mL}$) than carbendazim and prochloraz towards *B. cinerea* (MICs = 8 $\mu\text{g}/\text{mL}$) (Table 3). *B. cinerea* attacks more than 200 crops of economic importance and represents one of the most extensively studied necrotrophic pathogens. *A. tubingensis* was evaluated as a potential biocontrol agent against *B. cinerea* (Zhao et al., 2018), and the isolation of compound 4 described herein may provide the chemical basis for its biocontrol efficacy.

3. Conclusions

In conclusion, chemical investigation of the fungal strain *A. tubingensis* OUCMBIII 143291 led to the isolation and identification of eight specialised metabolites, including two undescribed diketopiperazine heterodimers, asperazine B (2) and C (3), and an undescribed 2-benzylpyridin-4(1H)-one-containing amide pestalamide D (4). It has been reported that *A. niger* and *A. tubingensis* are the two most representative species of black aspergilli, and due to their similar morphological characteristics and insufficient molecular identification, *A. tubingensis* has usually been misidentified as *A. niger*. This study firstly reported the isolation of asperazine from *A. tubingensis*. Furthermore, asperazines B (2) and C (3) were characterized as additional chemical markers distinguishing *A. tubingensis* from other related strains, providing a powerful tool for the rapid identification of black aspergilli. In addition, the undescribed compound 4 exhibited significant activity against the necrotrophic pathogen *B. cinerea*, which may reveal the chemical basis of the biocontrol efficacy of *A. tubingensis*.

4. Experimental section

4.1. General experimental procedures

Optical rotations were measured with a Jasco P-1020 digital polarimeter. UV spectra were obtained with a Shimadzu UV-2700 spectrophotometer. ECD spectra were collected with a Jasco J-815-150S circular dichroism spectrometer. Standard 1D and 2D NMR spectra were recorded on an Agilent DD2 500 MHz NMR spectrometer (500 and 125 MHz for ^1H and ^{13}C , respectively) with TMS as internal standard. HRESIMS spectra were measured on an LTQ Orbitrap XL spectrometer. Commercially available silica gel (100–200 mesh and 200–300 mesh, Qingdao Marine Chemical Co.), Lobar LiChroprep RP-18 (40–60 μm , Merck), and Sephadex LH-20 (Merck) were used for open column chromatography (CC). Precoated silica gel GF₂₅₄ plates were used for analytical TLC. All solvents used were either chemical or analytical grade.

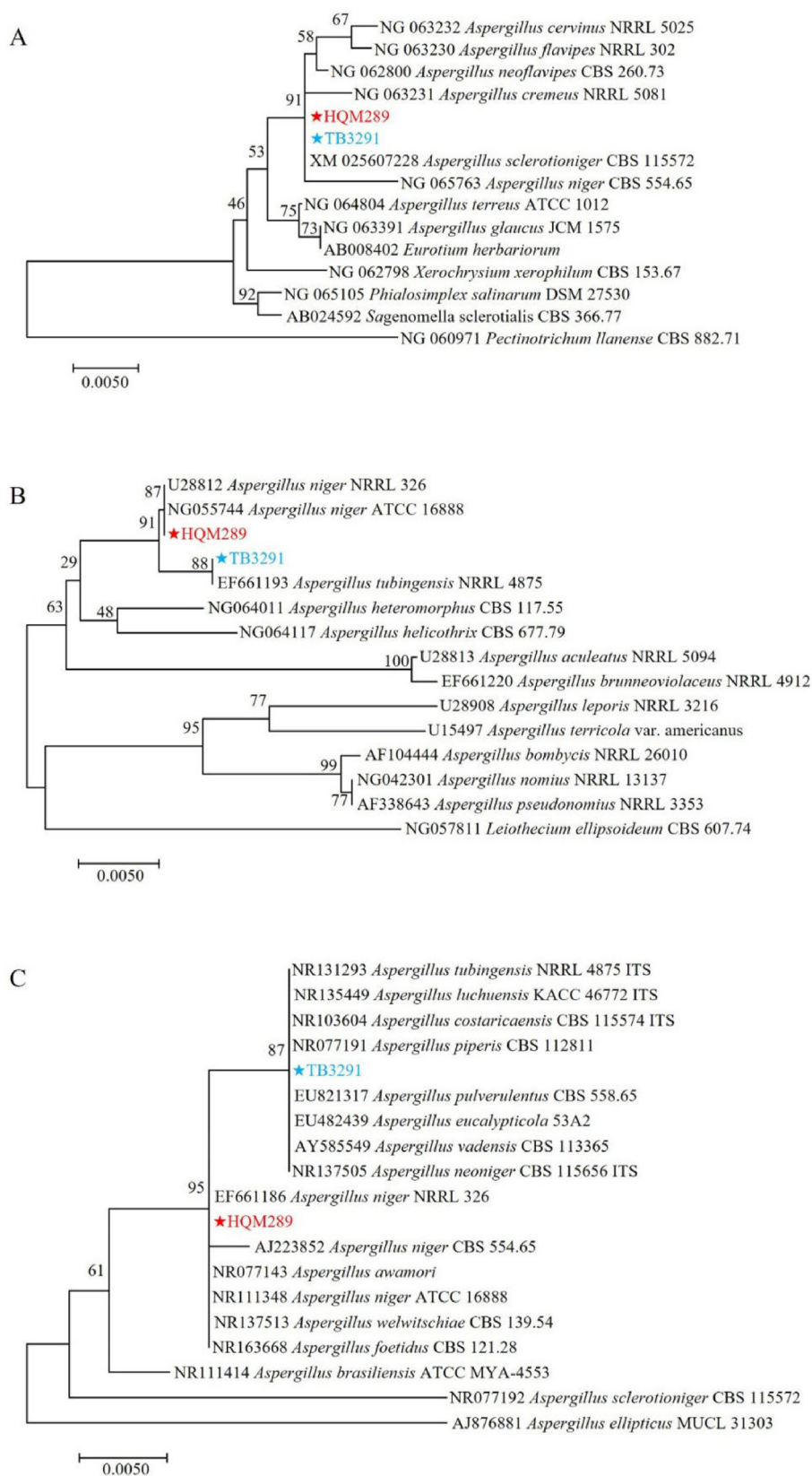


Fig. 6. Neighbor-joining (NJ) trees based on the 18S (A), 26S (B) and ITS rDNA regions (C). HQM289 and TB3291 represent *A. niger* and *A. tubingenensis*, respectively. NJ bootstrap values were estimated and marked above the branches.

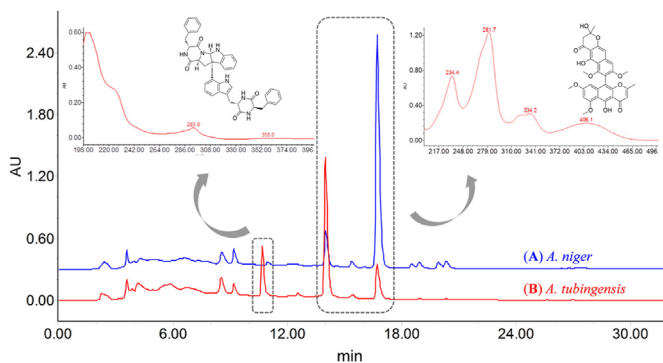


Fig. 7. HPLC-DAD spectra of the crude extracts of *A. niger* (A) and *A. tubingensis* (B) cultivated in PDB medium. (Chromatographic conditions: Column: SunFire® C18, 250 mm × 4.60 mm, 5 μm; Mobile phase: MeCN–H₂O, 0–30 min, 30%–100% MeCN; Flow rate: 1 mL/min; UV detection: 235 nm).

4.2. Fungal material and genomic DNA extraction

The fungal strains *Aspergillus niger* Tiegh. (Moniliaceae) and *Aspergillus tubingensis* Mosseray (Discellaceae) were previously isolated from the intertidal sediment sample, collected in Dongying, China (longitude 119°08'E; latitude 37°45'N), in June 2014. Morphologically, their black colonies enabled them to be easily classified as species of black aspergilli. Next, molecular reidentification was carried out. Both strains were cultured for 3 days at 28 °C under shaking conditions of 120 rpm in PDB medium. The mycelia were harvested, ground into a fine powder with liquid nitrogen and stored at –80 °C. The genomic DNA of these fungi was extracted from the powder with a protocol adapted from the trimethyl ammonium bromide (CTAB) method (Gao et al., 2019). The genomic DNA concentration and quality were estimated using a Nanodrop 2000 (Thermo Fisher Scientific, Wilmington, MA). *A. niger* and *A. tubingensis* were preserved at the College of Marine Life Sciences, Ocean University of China, under voucher numbers HQM289 and OUCMBIII 143291, respectively.

4.3. PCR amplification, DNA sequencing and phylogenetic analysis

To infer the evolutionary locations of these two isolated strains, we performed phylogenetic analysis using the sequences of the internal transcribed spacer rDNA (ITS region) and the 18S and 26S ribosomal RNA genes of these two species, together with those from the other *Aspergillus* species (Table S1), respectively. Detailed operating procedures including the information of the primers were presented in the Supplementary data. After PCR amplification, these three amplicons were separated and then sequenced by the Sanger method. Subsequently, the ITS rDNA and 18S and 26S rRNA sequences were aligned with those of other known species using Mega 6. Then, the alignments were used to construct the phylogenetic tree with Mega 6 using the

neighbor-joining (NJ) model. Branch confidences were estimated based on 1000 bootstrap replications for each gene.

4.4. Fermentation, extraction, and isolation

The fungal strain was cultivated in 100 × 1 L Erlenmeyer flasks, each containing 300 mL of modified PDB liquid medium (2% mannitol, 1% glucose, 0.3% peptone, 0.5% yeast extract, and 300 mL of naturally sourced and filtered seawater). Static fermentation was carried out for 30 days at room temperature. Afterwards, the fresh mycelia and culture broth were homogenized and then exhaustively extracted three times with EtOAc. The filtrates were evaporated under reduced pressure at 45 °C to afford 12 g of soluble crude extract. Initial chromatographic separation of the crude extract was performed by vacuum liquid chromatography (VLC) on silica gel, eluting with mixed petroleum ether (PE)–EtOAc and dichloromethane (DCM)–MeOH to give five fractions (Frs. 1–5). Since the HPLC-DAD spectrum of Fr. 3 (eluted with PE–EtOAc 1:1, v/v) contained absorptions characteristic of asperazine, this fraction was further purified by reversed-phase CC on Lobar LiChroprep RP-18 with a stepwise MeOH–H₂O gradient (from 1:9 to 10:0) to give five subfractions (Frs. 3.1–3.5). Fr. 3.1 (1.0 g) was further purified by silica gel eluting with a DCM–MeOH gradient (from 30:1 to 10:1) and then by Sephadex LH-20 (MeOH) to obtain compounds 7 (13.6 mg) and 8 (10.5 mg). Fr. 3.2 (38 mg) was subjected to Sephadex LH-20 (MeOH) and silica gel (DCM–acetone 2:1, v/v) CC to yield compounds 4 (3.9 mg) and 6 (5.5 mg). Fr. 3.3 (95 mg) was separated on silica gel (PE–EtOAc 1:1, v/v) to yield compound 5 (7.2 mg). Further purification of Fr. 3.4 (120 mg) by preparative TLC (pTLC; plate size, 20 × 20 cm; precoating, GF₂₅₄; developing solvents, DCM–MeOH, 20:1) and then by Sephadex LH-20 (MeOH) afforded compounds 1 (7.8 mg) and 2 (20.0 mg). Finally, compound 3 (4.0 mg) was isolated from Fr. 3.5 (60 mg) by silica gel (DCM–acetone 5:1, v/v) and Sephadex LH-20 (MeOH).

4.4.1. Asperazine B (2)

White amorphous powder; $[\alpha]_{25}^D +80$ (c 0.5, MeOH); UV (MeOH) λ_{\max} (log ϵ) 224 (4.20), 286 (3.91), 303 (3.92); ¹H and ¹³C NMR data, see Table 1; ESI HRMS at m/z 681.2812 [M + H]⁺ (calcd for C₄₀H₃₇N₆O₅, 681.2820).

4.4.2. OAsperazine C (3)

White amorphous powder; $[\alpha]_{25}^D +57$ (c 0.6, MeOH); UV (MeOH) λ_{\max} (log ϵ) 225 (4.36), 286 (4.01), 301 (4.00) nm; ¹H and ¹³C NMR data, see Table 1; ESI HRMS at m/z 665.2866 [M + H]⁺ (calcd for C₄₀H₃₇N₆O₄, 665.2871).

4.4.3. Pestalamide D (4)

Colorless oil; $[\alpha]_{25}^D -10$ (c 0.4, MeOH); UV (MeOH) λ_{\max} (log ϵ) 246 (4.04), 311 (4.01) nm; ¹H and ¹³C NMR data, see Table 2; ESI HRMS at m/z 357.1438 [M + H]⁺ (calcd for C₁₉H₂₁N₂O₅, 357.1445) and m/z 379.1255 [M + Na]⁺ (calcd for C₁₉H₂₀N₂O₅Na, 379.1264).

Table 3

Antifungal activities of compounds 1–8 (MIC, μg/mL).

no.	<i>A. alternata</i>	<i>A. brassicae</i>	<i>B. cinerea</i>	<i>C. lagenarium</i>	<i>F. oxysporum</i>	<i>G. graminis</i>	<i>P. digitatum</i>	<i>V. mali</i>
1	32	32	> 64	> 64	32	> 64	> 64	16
2	16	32	16	32	32	32	> 64	4
3	> 64	16	> 64	> 64	32	> 64	> 64	32
4	> 64	16	4	8	> 64	> 64	32	8
5	> 64	> 64	> 64	> 64	> 64	16	16	16
6	32	16	16	> 64	16	> 64	16	8
7	32	16	32	> 64	> 64	> 64	> 64	16
8	> 64	> 64	> 64	> 64	> 64	> 64	> 64	> 64
Ca*	8	8	8	4	4	4	4	4
Pr*	16	16	8	8	8	4	16	4

* Positive controls, carbendazim (Ca) and prochloraz (Pr).

4.5. Acidic hydrolysis of compounds 2 and 3 (Zhang et al., 2015)

Compounds 2 (2.2 mg) and 3 (3.0 mg) were separately hydrolyzed in HCl solution (6 mol/L, 10 mL) at 110 °C for 24 h. The hydrolysate was further evaporated under vacuum at 55 °C. The obtained residues were subjected to chiral HPLC analysis, which was performed with the aid of Daicel Chiral Technologies (China) Co., Ltd., through the following procedure: The samples were separately dissolved in mobile phase (pH 1.0 HClO₄ a. q.; final concentration of 1.0 mg/mL) and then analyzed on a Shimadzu LC-20A system equipped with a CROWNPAK® CR (+) column (CRPOCB-QB037) (0.40 cm I.D. × 15 cm L × 5 μm) and SPD-20A detector (205 nm). The injection volume was 8 μL, the flow rate was 0.4 mL/min, and the temperature was 25 °C. The presence of D-Tyr and D-Phe was confirmed by comparing the obtained retention times with those of standards (D-Tyr, 14.1 min; L-Tyr, 21.6 min; L-Phe, 25.9 min; D-Phe 38.0 min (Supporting Information)). Standard amino acids were purchased from Shanghai Yuanye Bio-Technology Co., Ltd.

4.6. Antifungal assay

The antifungal activity of the isolated compounds 1–8 against eight phytopathogenic fungi (*Alternaria alternata*, *Alternaria brassicae*, *Botrytis cinerea*, *Colletotrichum lagenarium*, *Fusarium oxysporum*, *Gaeumannomyces graminis*, *Penicillium digitatum*, and *Valsa mali*) were determined in 96-well microtitration plates with a modified method previously described in the literature (Xiao et al., 2014). All the plant pathogens were purchased from Qingdao Agricultural University (Qingdao, People's Republic of China). Carbendazim and prochloraz, ubiquitously applied as broad-spectrum fungicides in agriculture, were chosen as positive controls.

Author contributions

C. Xu and K. Xu contributed equally to this work.

Declaration of competing interest

The authors declare no competing financial interest.

Acknowledgments

This work was supported by the Agricultural Science and Technology Innovation Program (Grant No. ASTIP-TRIC04 and ASTIP-TRIC05) and Major Projects [No.110201601023 (LS-03) and 110201901040 (LS-03)].

Appendix A. Supplementary data

Supplementary data to this article can be found online at <https://doi.org/10.1016/j.phytochem.2020.112399>.

References

Abdel-Aziz, M.M., Emam, T.M., Elsherbin, E.A., 2019. Effects of Mandarin (*Citrus reticulata*) peel essential oil as a natural antibiofilm agent against *Aspergillus niger* in

- onion bulbs. *Postharvest Biol. Technol.* 156, 110959.
- Apaliya, M.T., Zhang, H., Yang, Q., Zheng, X., Zhao, L., Kwaw, E., Mahunu, G.K., 2017. *Hanseniaspora uvarum* enhanced with trehalose induced defense-related enzyme activities and relative genes expression levels against *Aspergillus tubingensis* in table grapes. *Postharvest Biol. Technol.* 132, 162–170.
- Barrow, C.J., Cai, P., Snyder, J.K., Sedlock, D.M., Sun, H.H., Cooper, R., 1993. WIN 64821, a new competitive antagonist to substance P, isolated from an *Aspergillus* species: structure determination and solution conformation. *J. Org. Chem.* 58, 6016–6021.
- Bathoorn, E., Salazar, N.E., Sepehrkhoy, S., Meijer, M., de Cock, H., Haas, P.J., 2013. Involvement of the opportunistic pathogen *Aspergillus tubingensis* in osteomyelitis of the maxillary bone: a case report. *BMC Infect. Dis.* 13, 59.
- Cao, F., Meng, Z.H., Mu, X., Yue, Y.F., Zhu, H.J., 2019. Absolute configuration of bioactive azaphilones from the marine-derived fungus *Pleosporales* sp. CF09-1. *J. Nat. Prod.* 82, 386–392.
- Choque, E., El Rayess, Y., Raynal, J., Mathieu, F., 2014. Fungal naphtho-γ-pyrone – secondary metabolites of industrial interest. *Appl. Microbiol. Biotechnol.* 99, 1081–1096.
- Choque, E., Klopp, C., Valiere, S., Raynal, J., Mathieu, F., 2018. Whole-genome sequencing of *Aspergillus tubingensis* G131 and overview of its secondary metabolism potential. *BMC Genom.* 19, 200–215.
- D'hooge, E., Becker, P., Stubbe, D., Normand, A.C., Piarroux, R., Hendrickx, M., 2019. Black aspergilli: a remaining challenge in fungal taxonomy? *Med. Mycol.* 57, 773–780.
- Ding, G., Jiang, L., Guo, L., Chen, X., Zhang, H., Che, Y., 2008. Pestalazines and pestalamides, bioactive metabolites from the plant pathogenic fungus *Pestalotiopsis theae*. *J. Nat. Prod.* 71, 1861–1865.
- Gao, Y., Li, L., Zhang, X., Wang, X., Ji, W., Zhao, J., Ozaki, Y., 2019. CTAB-triggered Ag aggregates for reproducible SERS analysis of urinary polycyclic aromatic hydrocarbon metabolites. *Chem. Commun.* 55, 2146–2149.
- Henrikson, J.C., Ellis, T.K., King, J.B., Cichewicz, R.H., 2011. Reappraising the structures and distribution of metabolites from black aspergilli containing uncommon 2-benzyl-4H-pyran-4-one and 2-benzylpyridin-4(1H)-one systems. *J. Nat. Prod.* 74, 1959–1964.
- Li, X.B., Li, Y.L., Zhou, J.C., Yuan, H.Q., Wang, X.N., Lou, H.X., 2015. A new diketopiperazine heterodimer from an endophytic fungus *Aspergillus niger*. *J. Asian Nat. Prod. Res.* 17, 182–187.
- Li, Y., Sun, K.L., Wang, Y., Fu, P., Liu, P.P., Wang, C., Zhu, W.M., 2013. A cytotoxic pyrrolidinoinodoline diketopiperazine dimer from the algal fungus *Eurotium herbariorum* HT-2. *Chin. Chem. Lett.* 24, 1049–1052.
- Mirhendi, H., Zarei, F., Motamedi, M., Nouripour-Sisakht, S., 2016. *Aspergillus tubingensis* and *Aspergillus niger* as the dominant black *Aspergillus*, use of simple PCR-RFLP for preliminary differentiation. *J. Mycol. Med.* 26, 9–16.
- Nielsen, K.F., Mogensen, J.M., Johansen, M., Larsen, T.O., Frisvad, J.C., 2009. Review of secondary metabolites and mycotoxins from the *Aspergillus niger* group. *Anal. Bioanal. Chem.* 395, 1225–1242.
- Ovenden, S.P.B., Sberna, G., Tait, R.M., Wildman, H.G., Patel, R., Li, B., Steffy, K., Nguyen, N., Meurer-Grimes, B.M., 2004. A diketopiperazine dimer from a marine-derived isolate of *Aspergillus niger*. *J. Nat. Prod.* 67, 2093–2095.
- Perrone, G., Susca, A., Cozzi, G., Ehrlich, K., Varga, J., Frisvad, J.C., Meijer, M., Noonim, P., Mahakarnchanakul, W., Samson, R.A., 2007. Biodiversity of *Aspergillus* species in some important agricultural products. *Stud. Mycol.* 59, 53–66.
- Samson, R.A., Noonim, P., Meijer, M., Houbraken, J., Frisvad, J., Varga, J., 2007. Diagnostic tools to identify black aspergilli. *Stud. Mycol.* 59, 129–145.
- Varga, J., Frisvad, J.C., Kocsubé, S., Brankovics, B., Tóth, B., Szigeti, G., Samson, R.A., 2011. New and revisited species in *Aspergillus* section *Nigri*. *Stud. Mycol.* 69, 1–17.
- Varoglu, M., Corbett, T.H., Valeriotte, F.A., Crews, P., 1997. Asperazine, a selective cytotoxic alkaloid from a sponge-derived culture of *Aspergillus niger*. *J. Org. Chem.* 62, 7078–7079.
- Xanthopoulou, A., Ganopoulos, I., Tryfinopoulou, P., Panagou, E.Z., Osathanunkul, M., Madesis, P., Kizis, D., 2019. Rapid and accurate identification of black aspergilli from grapes using high-resolution melting (HRM) analysis. *J. Sci. Food Agric.* 99, 309–314.
- Xiao, J., Zhang, Q., Gao, Y.Q., Tang, J.J., Zhang, A.L., Gao, J.M., 2014. Secondary metabolites from the endophytic *Botryosphaeria dothidea* of *Melia azedarach* and their antifungal, antibacterial, antioxidant, and cytotoxic activities. *J. Agric. Food Chem.* 62, 3584–3590.
- Zhang, P., Li, X.M., Wang, J.N., Li, X., Wang, B.G., 2015. Prenylated indole alkaloids from the marine-derived fungus *Paecilomyces variotii*. *Chin. Chem. Lett.* 26, 313–316.
- Zhao, J., Liu, W., Liu, D., Lu, C., Zhang, D., Wu, H., Dong, D., Meng, L., 2018. Identification and evaluation of *Aspergillus tubingensis* as a potential biocontrol agent against grey mould on tomato. *J. Gen. Plant Pathol.* 84, 148–159.